<u>**Original Article**</u>

A THERMALLY RESPONSIVE SHORT ELASTIN LIKE POLYPEPTIDE-DRUG CONJUGATE: SYNTHESIS, CHARACTERIZATION AND BIOLOGICAL EVALUATION FOR TARGETED DELIVERY OF ANTICANCER DRUGS

RUBHA SAXENA, MOOLA JOGHEE NANJAN*,

TIFAC CORE HD, J. S. S. College of Pharmacy, (Off Campus, JSS University, Mysore) Ootacamund, The Nilgiris 643001, Tamil Nadu, India. Email: mjnanjan@gmail.com

ABSTRACT

Introduction: Among the several new strategies explored today to avoid the side effects in cancer chemotherapy. The concept of polymer-drug conjugates has shown considerable promise. In this context, genetically engineered long elastin like polypeptides (ELPs) have been examined recently as drug carriers. These ELPs, however, have certain limitations.

Objective: It is our hypothesis that short synthetic ELPs can also be used as drug carriers so as to overcome these limitations. The purpose of this investigation was, therefore, to synthesize, characterize and evaluate a thermally responsive short ELP-Doxorubicin conjugate for targeted delivery.

Methods: The ELP-Doxorubicin conjugate of molecular weight 1280 Da was synthesized and characterized by ESI-MS, FTIR and NMR studies. Turbidimetry, differential scanning calorimetry (DSC) and circular dichorism (CD) studies were carried out to evaluate its structural transition behavior. Cellular uptake and intracellular localization studies of the conjugate and the free drug were carried out by flow cytometry and confocal fluorescence microscopy, respectively. *In vitro* cytotoxicity of the conjugate was evaluated by the MTT assay method and compared with that of the free drug.

Results: The results reveal that the short ELP synthesized exhibits structural transition behavior similar to naturally occurring long ELPs and delivers more drug molecules to intracellular space compared to the free drug. This structural transition behavior can also be exploited for targeting drugs to solid tumors using hyperthermia.

Conclusion: As hypothesized our investigations clearly demonstrate that short thermally responsive ELPs are good carrier for targeting anticancer drugs to the intracellular space.

Keywords: Anticancer drug, Drug delivery system, Drug targeting, Elastin like polypeptide, Drug conjugate.

INTRODUCTION

Mortality due to cancer is rising continuously the world over. Further, it is becoming very clear that the objective of developing specific low molecular weight drugs capable of preventing tumor growth without causing non-specific side effects is not possible [1]. Approaches are, therefore, being made today to improve the existing therapies like identifying new tumor specific molecular targets through genomics and proteomics and developing innovative drug delivery systems to target drugs to tumor cells and away from sites of toxicity in addition to maintaining the therapeutic concentration of drugs over long periods of time [2-5].

Among the several new strategies of drug delivery systems being developed today, the concept of polymer-drug conjugates has shown considerable promise. Several of these conjugates are in different phases of clinical trials for various cancers [6]. In this context, genetically engineered long elastin like polypeptides (ELPs) have also been examined as drug carriers. These are pentapeptide repeats of Val-Pro-Gly-Xaa-Gly amino acids (VPGXaaG)$_n$, where Xaa is a guest residue (except Pro) and n may vary from 10 to 200. These peptides are biocompatible, biodegradable, non immunogenic and can retain in blood circulation for longer times [7-12]. In addition to passively targeting to tumors by the enhanced permeable and retention (EPR) effect, they also show improved cytotoxicity in multidrug resistant cell lines compared to the free drug because of their longer plasma half-lives [13]. Another important feature of ELPs is their capability to undergo inverse temperature transition (ITT) behavior, which can be exploited by the application of external hyperthermia to induce these to localize in tumors. Investigations have, therefore, been carried out using genetically engineered ELPs for developing ELP-drug conjugates [14-16].

In all these investigations, genetically engineering techniques have been used for synthesizing the ELPs. This technique, however, is cumbersome and expensive. The presence of reactive side chain in these ELPs also makes them unstable over long periods of time and at higher temperatures. There is a need, therefore, to develop more versatile chemical approaches that require fewer synthetic steps. In this context, it is our hypothesis that short synthetic ELPs can also be used as drug carriers. They offer the possibility of higher amounts of drug conjugation. Further, it has been shown that short synthetic ELPs also undergo ITT behavior like genetically engineered long ELPs thus showing that pentameric repeat units are not always necessary for this behavior [17-18]. A detailed literature survey, however, revealed that such short synthetic ELPs, have not been investigated so far for developing and evaluating their drug conjugates.

The aim of the present investigation was, therefore, to synthesize a short ELP, namely GVGVPGVG, and evaluate its potential for targeted delivery of anticancer drugs by *in vitro* methods. Doxorubicin (Dox) was selected for conjugation as it is commonly used in the treatment of a wide range of cancers, hematological malignancies, many types of carcinoma and soft tissue sarcomas [19-20]. The mode of action of Dox is to block the synthesis of DNA by intercalating into the DNA strand and inhibit DNA topoisomerase II synthesis. Further, the C-13 position of Dox can be exploited for linking the short ELP through an acid labile hydrolyzable linkage, namely hydrazone (C=N-NH). A hydrolysable linkage is important for releasing the drug inside the lysosomal compartments of the cell. Water soluble polymeric drug conjugates are known to be taken in by cells by pinocytosis and trafficked via the endosomal compartments to the lysosomal compartments. The lysosomal enzymes at their acidic pH hydrolyze the acid sensitive hydrazone bond of the ELP-Dox conjugate and liberate the free drug, Dox. The free drug will then diffuse from the lysosomes into the cytoplasm and cause cell lysis/apoptosis.
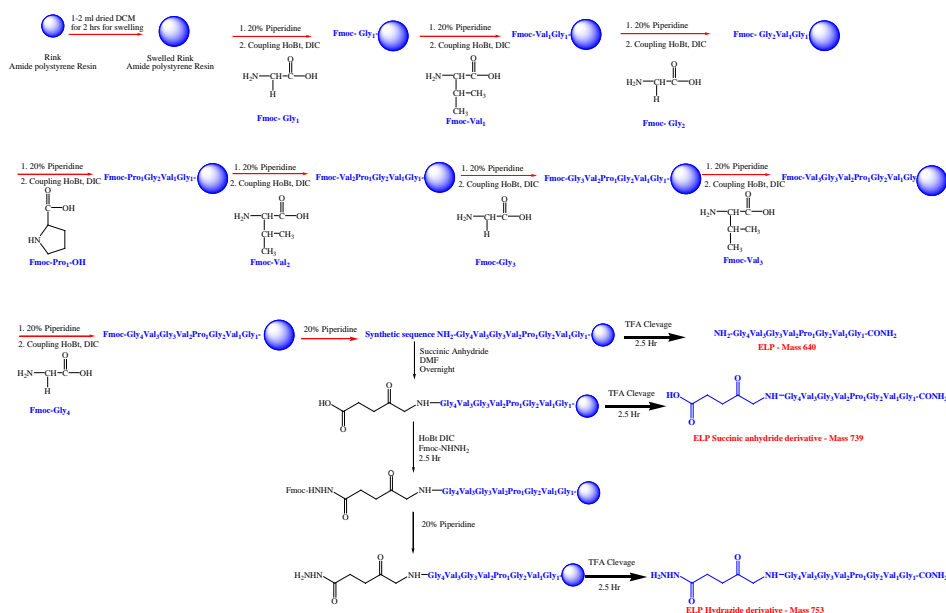
MATERIALS AND METHODS

Rink amide (amino methyl) polystyrene resin (loading capacity ~1.0 mmol/g), Fmoc-Val, Fmoc-Gly and Fmoc-Pro-OH, succinic anhydride, triple distilled water, PBS and acetonitrile were procured from Fluka. Piperidine, HoBt, DIC, and diethyl ether were obtained from Spectrochem. Triisopropyl silane, 1-2 ethanedithiol, phenol, ninhydrin, trifluroacetic acid, anhydrous methanol, Fmoc hydrazide, Dox (>99%), Dulbecco's Minimum Essential Medium (DMEM), penicillin G, streptomycin, nystatin, dimethyl sulfoxide (DMSO), dihydroethidium (DHE), DMSO d_6 were procured from Sigma Aldrich.

General methods

^{1}H NMR and ^{13}C NMR spectra were recorded on Bruker 400 spectrometer. ESI-MS was performed on Micromass Q-TOF mass spectrometer electron spray ionization mode. IR spectra were recorded by FTIR model Thermo-iCAP 6000 Series. High performance liquid chromatography (HPLC) was performed on LC-

2010HT - Shimadzu system, using aqueous acetonitrile solution containing 0.05% TFA as a mobile phase and C-18 column, 4.6X250 mm Kromasil C-18 column. Sample solution was eluted with a linear gradient of aqueous acetonitrile at a flow rate of 1 ml/min and detected by UV absorbance at the wavelength 220 nm. The HPLC purified samples were subjected to lyophilization to remove the excess solvent with the help of ALPHA 1-2 LD lyophilizer.
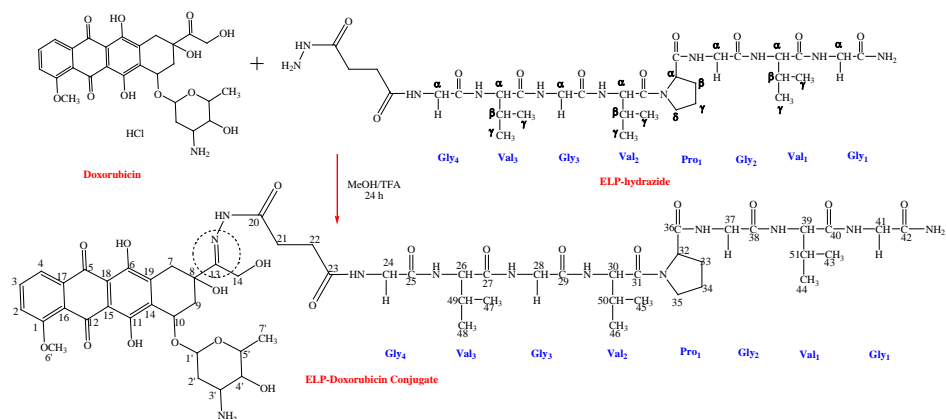
A short ELP, H-Gly$_4$-Val$_3$-Gly$_3$-Val$_2$-Pro$_1$-Gly$_2$-Val$_1$-Gly$_1$-NH$_2$, was synthesized by Merrifield solid phase peptide synthetic technique using Fmoc chemistry on rink amide (amino methyl) polystyrene resin (loading capacity ~1.0 mmol/g) as shown in Scheme 1. The Fmoc group was deprotected from the last coupled amino acid, namely Gly$_4$ using 20% piperidine solution. Succinic anhydride was then added to obtain the succinic anhydride derivative of the ELP. The Fmoc hydrazide was added to the succinic anhydride derivative to obtain the ELP-hydrazide. Cleavage of the peptides from the resin and their precipitation and purification by reverse phase HPLC were achieved by standard procedures [21].

Scheme 1: Solid phase peptide synthesis of short ELP

ELP-hydrazide was then coupled to Dox via the acid sensitive hydrolysable hydrazone linkage at the C-13 position of Dox as shown in Scheme 2. Dox (0.0017 mmol) and ELP-hydrazide (0.0051 mmol) were dissolved in anhydrous methanol. Trifluoroacetic acid was then added to catalyze the reaction. The reaction mixture was stirred at room temperature for 24 h while being protected from

light. After 24 h the reaction was complete. The solvent was then removed under vacuum at room temperature. The residue was mixed with a small amount of methanol and placed in ultrasonic bath for 5 min. Chilled diethyl ether was added slowly when a red solid product, ELP-Dox conjugate, precipitated. It was collected by centrifugation and dried under vacuum.

Scheme 2: Solution phase coupling of Dox to the short ELP

Structural characterization of the ELP, its derivatives and the ELP-Dox conjugate was carried out by ESI-MS, FTIR, ^{1}H NMR and ^{13}CNMR. The ITT of the short ELP was determined by measuring the optical turbidity of its aqueous solution as a function of temperature using Varion D spectrophotometer, Bio-Logic MOS-450/AF, equipped with multi cell thermoelectric temperature controller. The purified ELP was dissolved in PBS buffer (1 M, pH= 7.2) in the concentration range of 0.5-5 mg/ml. The turbidity profile was obtained by heating a 100 μm solutions of the ELP and measuring the transmission at 240 nm as a function of temperature at 2^0C/min heating scan rate.

The physical and structural transition behavior of the short ELP was assessed by DSC and CD. A quantity of 20 μl (3.5 mg/ml) of the ELP solution in PBS (pH 7.2) was placed in a 40 μl aluminum pan of DSC (Mettler Toledo) and hermetically sealed. An equal volume of PBS (pH 7.2) was placed in the reference pan. The ELP was heated at a scanning rate of 2^0C/min from 25^0C to 180^0C using calorimetric program consisting of a pre-equilibration phase at 20^0C for 20 min. The CD spectrum of the ELP (100 μm) in PBS at 7.2 pH was recorded on JASCO J-710 spectropolarimeter under constant nitrogen flush. CD scans were performed at three different temperatures, allowing the sample to equilibrate at each temperature for 5 min under constant nitrogen flush. The cuvette temperature was measured with Peltier equipped thermometer. The scans were collected using a spectral acquisition spacing of 0.5 or 1.0 nm (with 2.0 nm bandwidth) with an integration time of one second from 190 up to 260 nm. Scans were processed on a computer and the average of 4 runs was taken.

The cerebral glioma cell lines (BMG-1; diploid, wild type p53) were cultured in Dulbecco's Minimum Essential Medium (DMEM) with 5% foetal bovine serum containing the antibiotics, penicillin (100 units/ml), streptomycin (50 units/ml) and nystatin (2 g/ml) in humidified 5% CO_2 incubator at 37^0C for in vitro MTT cell viability assay, flow cytometry and confocal fluorescence microscopy studies.

The monolayer cell culture was trypsinized and the cell count adjusted to 5000 cells/200 μl/well. After 24 h, when a partial monolayer was formed, the supernatant was flicked off and the monolayer washed with the medium. Different concentrations of Dox and the ELP-Dox conjugate (5, 10, 20 50 100 μm each) were added to microtitre plates. The plates were then incubated at 37^0C for 3 days in 5% CO_2 atmosphere. Microscopic examination was carried out and observations were noted every 24 h. The medium was discarded and 20 μl of MTT in PBS was added to each well. The plates were further incubated for 2 h while being protected from light at room temperature to solubilize the formazan formed. The absorbance was measured using a microplate reader at the wavelength of 540 nm. The percentage growth inhibition was calculated using formula,

$$\% \text{ Growth Inhibition} = 100 - \left(\frac{\text{Mean OD of individual test group}}{\text{Mean OD of control group}} \times 100 \right)$$

OD is the optical density measured at 540 nm. The experiment was performed twice.

Flow cytometry was performed to quantify the relative fluorescence intensity of Dox and the ELP-Dox conjugate using various detectors. In order to check the membrane integrity of BMG-1 (diploid, wild type p53) cells, $\sim 10^6$ cells at log phase were mixed separately with the free drug, Dox and the ELP-Dox conjugate (100 μm) and incubated at 37^0C for 24 h with constant shaking. The cells were collected, washed twice with PBS in a petridish (5×10^6cells/dish) and resuspended in PBS for flow cytometric analysis under FACS LSR II flow cytometer. Fluorescence intensity of each cell was recorded and processed to obtain the histogram describing the distribution of the relative fluorescence unit (RFU) amongst the live cells. The free drug and the ELP-Dox conjugate treated cell groups along with the control group were analyzed. A gate corresponding to control cells was assigned based on the forward-scatter/side-scatter plot.

In order to demonstrate the intracellular distribution of the fluorescent Dox and the ELP-Dox conjugate, BMG-1 cells were first grown on sterile glass cover slips in petridish (5×10^6cells/dish). After 24 h, the cells were washed with serum free medium, treated separately with 100 μm of Dox and the ELP-Dox conjugate (prepared in DMEM serum free medium prior to use) and incubated at 37^0C. At the end of the treatment, the cells were washed with PBS and examined under confocal fluorescence microscope and the images were captured using 40X objective.

RESULTS AND DISCUSSION

A thermally responsive short ELP was synthesized using solid phase peptide synthesis. Dox was successfully conjugated to the ELP via the hydrazone linkage at the C-13 position of Dox as outlined in Schemes 1 and 2.

The ESI-MS mass spectra showed molecular ion peak at m/z 640.04 Da, 740.5 Da, 754.9 Da and 1280.4 Da consistent with the molecular formula $C_{28}H_{48}N_8O_9$, $C_{32}H_{53}N_9O_{11}[M+1H]$, $C_{32}H_{55}N_{11}O_{10}[M+1H]$ and $C_{59}H_{82}N_{12}O_{20}[M+1H]$ for ELP, ELP succinic anhydride, ELP-hydrazide and ELP-Dox conjugate, respectively (Table 1).

Table 1: Molecular weights estimated by ESI-MS

Sample	Molecular Formula	Expected Molecular Mass [M] (Dalton)	Observed Molecular Mass (Dalton)
ELP	$C_{28}H_{48}N_8O_9$	640.73 Da	640.2 Da [M+1H]
ELP-succccinic anhydride	$C_{32}H_{53}N_9O_{11}$	739.82 Da	740.5 Da [M+1H]
ELP-hydrazide	$C_{32}H_{55}N_{11}O_{10}$	753.85 Da	754.9 Da [M+1H]
ELP-Dox conjugate	$C_{59}H_{82}N_{12}O_{20}$	1279.35 Da	1280.4 Da [M+1H]

The series of characteristic IR bands obtained in FTIR spectra for Dox, ELP, ELP-hydrazide and ELP-Dox conjugate are summarized in Table 2. The data reveal a new band at 1653 cm^{-1} for the ELP-Dox conjugate that may be assigned to the stretching (υ C=N) vibrations which corresponds to the disappearance of Dox alkyl carbonyl group (C-13) and the formation of the drug conjugate with the new C=N linkage (Fig. 1).

Table 2: Assignment of FTIR spectral peaks for ELP-Dox conjugate

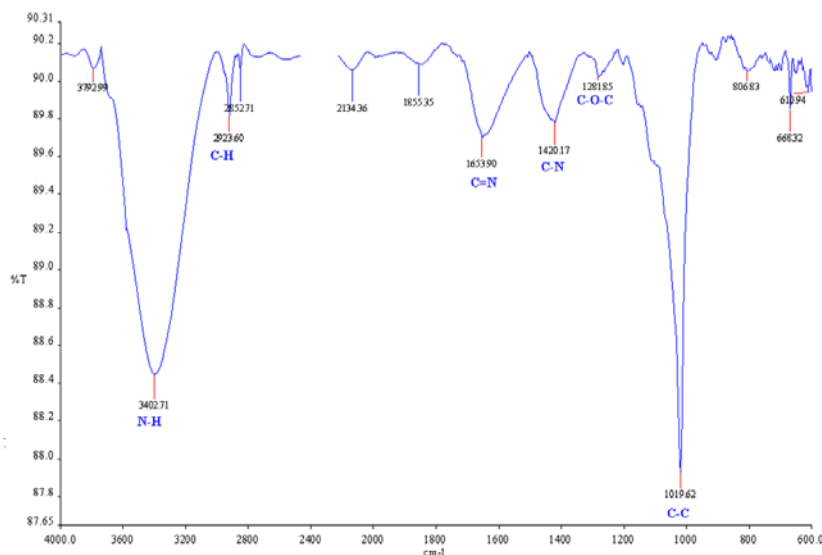| Sample	IR Bands cm^{-1}	Description
ELP-Dox conjugate	3402	υ (N-H)
	3326	υ (H-O)
	2923	υ (C-H)
	1653	υ (C=N)
	1420	υ (C-N)
	1281	υ (C-O-C)
	1019	υ (C-C)

Fig. 1: FTIR spectra for ELP-Dox conjugate

The ^{1}HNMR data obtained are good in agreement for the structure of ELP-Dox conjugate: δ = 3.71 (d, J=8 Hz, 1H, Gly$_4$ - α - CH$_a$), 3.67 (d, J=8 Hz, 1H, Gly$_4$ - α - CH$_b$), 8.22 (t, J=4 Hz, 1H, Gly$_4$ - α - NH), 0.80 (d, J=7.5 Hz, 3H, Val$_3$ - γ - CH$_{3a}$), 0.82 (d, J=7.5 Hz, 3H, Val$_3$ - γ - CH$_{3b}$), 1.95 (m, 1H, Val$_3$ - β - CH), 4.28 (dd, J=8 Hz, 1H, Val$_3$ - α - CH), 8.21 (d, J=4 Hz, 1H, Val$_3$ - α - NH), 3.67 (d, J=8 Hz, 1H, Gly$_3$ - α - CH$_a$), 3.65 (d, J=8 Hz, 1H, Gly$_3$ - α - CH$_b$), 8.20 (t, J=4 Hz, 1H, Gly$_3$ - α - NH), 0.83 (d, J=7.5 Hz, 3H, Val$_2$ - γ - CH$_{3a}$), 0.84 (d, J=7.5 Hz, 3H, Val$_2$ - γ - CH$_{3b}$),), 1.94 (m, 1H, Val$_2$ - β - CH), 4.28 (dd, J=8 Hz, 1H, Val$_2$ - α - CH), 7.91 (d, J=8 Hz, 1H, Val$_2$ - α - NH), 4.13 (bt, J=8 Hz, 1H, Pro$_1$ - α - CH), 1.94 (m, 2H, Pro$_1$ - β - CH$_2$), 1.88 (m, 2H, Pro$_1$ - γ - CH$_2$), 3.72 (t, J=8 Hz, 2H, Pro$_1$ - δ - CH$_2$), 3.67 (d, J=8 Hz, 1H, Gly$_2$ - α - CH$_a$), 3.65 (d, J=8 Hz, 1H, Gly$_2$ - α - CH$_b$), 7.89 (t, J=8 Hz, 1H, Gly$_2$ - α - NH), 0.87 (d, J=7.5 Hz, 3H, Val$_1$ - γ - CH$_{3a}$), 0.89 (d, J=7.5 Hz, 3H, Val$_1$ - γ - CH$_{3b}$),), 1.97 (m, 1H, Val$_1$ - β - CH), 4.28 (dd, J=8 Hz, 1H, Val$_1$ - α - CH), 7.67 (d, J=8 Hz, 1H, Val$_1$ - α - NH), 3.71 (d, J=8 Hz, 1H, Gly$_1$ - α - CH$_a$), 3.72 (d, J=8 Hz, 1H, Gly$_1$ - α - CH$_b$), 7.97 (t, J=8 Hz, 1H, Gly$_1$ - α - NH), 3.60 (d, J=4 Hz, 2H, 21-H), 3.56 (d, J=4 Hz, 2H, 22-H), 7.81 (d, J=8 Hz, 1H, 4-H), 7.65 (d, J=8 Hz, 1H, 3-H), 7.67 (d, J=8 Hz, 1H, 2-H), 5.42 (s, 1H, 1′-H), 5.29 (s, 1H, 8-OH), 4.30 (s, 1H, 10-H), 4.56 (s, 1H, 5′-H), 4.13 (s, 1H, 4′-H), 3.98 (s, 1H, 1-OCH$_3$), 3.72 (s, 1H, 3′-H), 2.42 (dd, J=16Hz, 1H, 7-eqH), 2.40 (dd, J=16Hz, 1H, 7-axH), 2.14 (m, 1H, 9-eqH), 2.37 (m, 1H, 9-axH), 1.82 (t, J=12Hz, 1H, 2′-eqH), 1.83 (t, J=12Hz, 1H, 2′-axH), 1.15 (s, 1H, 5′-CH$_3$) (Fig. 2).
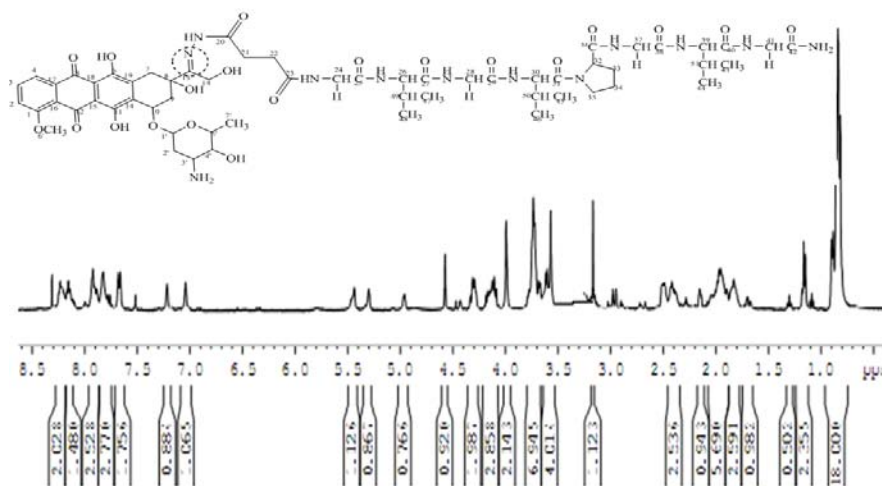

Fig. 2: ^{1}HNMR for ELP-Dox conjugate

The ^{13}C NMR data obtained are in good agreement for the structure of ELP-Dox conjugate: δ = 160.82 (C-1), 119.04 (C-2), 134.16 (C-3), 119.80 (C-4), 186.72 (C-5), 155.97 (C-6), 32.05 (C-7), 74.76 (C-8), 32.05 (C-9), 74.76 (C-10), 155.97 (C-11), 188.82 (C-12), 155.97 (C-13), 135.23 (C-14), 110.76 (C-15), 119.80 (C-16), 135.23 (C-17), 110.69 (C-18), 135.23 (C-19), 99.13 (C-1′), 28.73 (C-2′), 46.59 (C-3′), 66.13 (C-4′), 66.06 (C-5′), 57.74 (C-6′- OCH$_3$), 16.67 (C-7′-CH$_3$), 168.50 (C-20), 30.32 (C-21), 30.24 (C-22), 171.12 (C-23), 42.12 (Gly$_4$ - α - C), 170.94 (Gly$_4$ - C=O), 19.11 (Val$_3$ - γ - C), 29.08 (Val$_3$ - β - C), 58.23 (Val$_3$ - α - C), 170.81 (Val$_3$ - C=O), 42.12 (Gly$_3$ - α - C), 170.81 (Gly$_3$ - C=O), 18.43 (Val$_2$ - γ - C), 29.08 (Val$_2$ - β - C), 58.23 (Val$_2$ - α - C), 170.81 (Val$_2$ - C=O), 66.65 (Pro$_1$ - α - C), 28.15 (Pro$_1$ - β - C), 24.42 (Pro$_1$ - γ - C), 47.23 (Pro$_1$ - δ - C), 41.76 (Gly$_2$ - α - C), 168.92 (Gly$_2$ - C=O), 18.20 (Val$_1$ - γ - C), 29.18 (Val$_1$ - β - C), 63.65 (Val$_1$ - α - C), 169.98 (Val$_1$ - C=O), 41.60 (Gly$_1$ - α - C), 169.98 (Gly$_1$ - C=O).

^{13}C NMR data also reveal that the chemical shift of the C-13 carbonyl carbon of Dox shifts from 214.42 ppm to 155.97 ppm thus confirming that Dox is coupled to the ELP via the hydrazone linkage (Fig. 3).
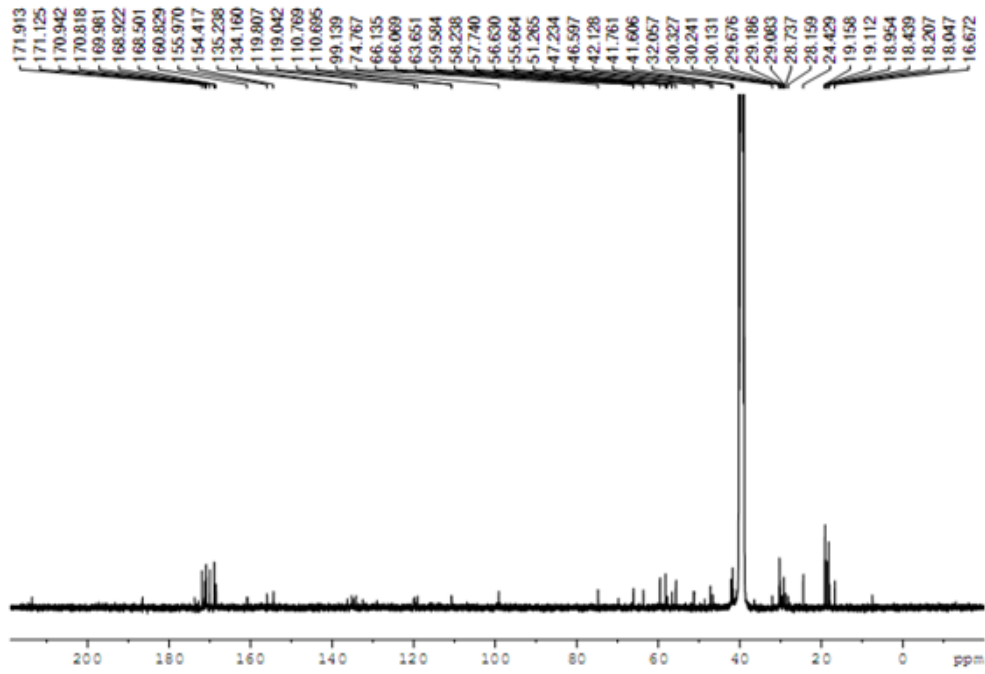
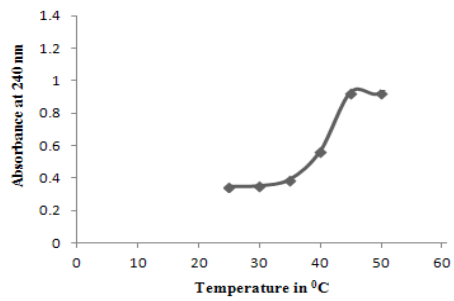**Fig. 3: ^{13}C NMR for ELP-Dox conjugate**

Fig. 4: Turbidity profile for ELP (optical density at 240 nm) as a function of temperature

The turbidity profile of the ELP as a function of temperature is shown in Fig. 4. The results reveal that the ELP is soluble in aqueous solution at 37^0C but as the temperature increases it starts aggregating above 40^0C, its ITT. Below its ITT the ELP is a clear solution but upon heating the solution becomes turbid because of the aggregation of the ELP. It exhibits a single narrow ITT over a 1-2^0C range. The short ELP thus exhibits an ITT behavior near the physiological temperature (37 ± 3^0C).

The DSC thermogram of the ELP is shown in Fig. 5. The figure indicates a clear visualization of the physical transition of the ELP. An exothermic peak near 40^0C observed denotes the peak temperature, T_p, which corresponds to the phase transition. The thermogram also shows a glass transition for the ELP at 97^0C, corresponding to the degeneration of ELP at higher temperatures.
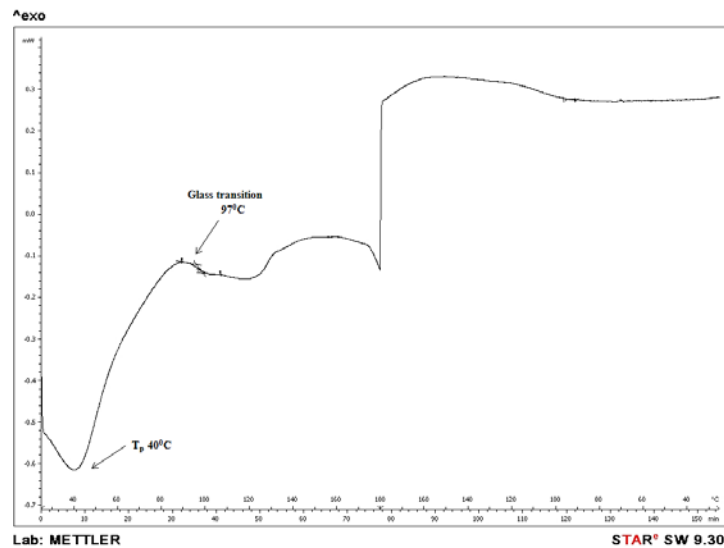

Fig. 5: DSC thermogram for ELP

The thermally induced structural transition behavior of the ELP was also examined by CD studies at three different temperatures, namely room temperature (27⁰C), physiological temperature (37⁰C) and ITT (40⁰C). The CD spectra obtained is shown in Fig. 6. The spectra reveals that the short ELP at 100 µm concentration in PBS buffer of pH 7.2 undergoes a secondary structural transition with respect to temperature change. At 27⁰C the CD spectrum consists of a large negative dip at 197 nm and a small shallow minimum dip at 220 nm corresponding to random structure of the ELP. As the temperature increases a shift in the band from 197 nm to 199 nm occurs, whereas the shallow minimum band at 220 nm increases concomitantly. The temperature dependent CD results are thus in good agreement with the existence of two main conformational states, namely one dominating at low temperatures consisting of random structure and the other prevailing at higher temperatures consisting of type II β turns. This behavior is similar to genetically engineered long ELPs.
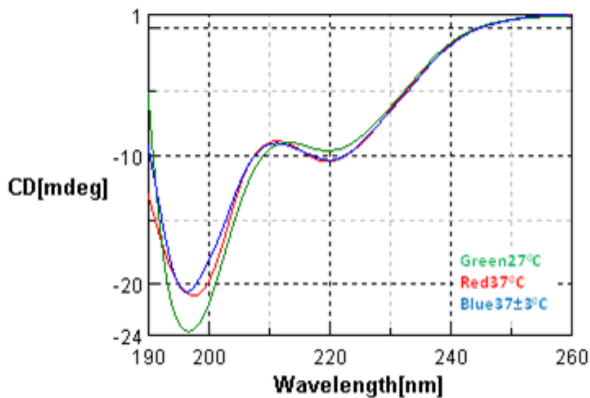
metabolism of MTT. The results obtained are shown in Fig. 7. The results reveal that the ELP does not exhibit any intrinsic cytotoxicity. At 24 and 72 h, Dox and ELP-Dox conjugate show almost similar, approximately 42% and 78%, growth inhibition, respectively.
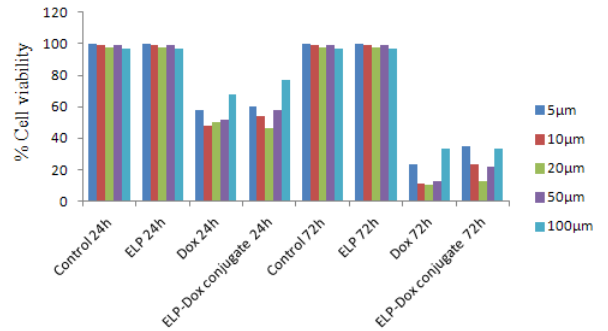

Fig. 7: Cytotoxicity effect of ELP, Dox and ELP-Dox conjugate on BMG-1 cell lines

The cellular uptake of Dox and the ELP-Dox conjugate by BMG-1 cerebral glioma cell line was measured using flow cytometry after 24 h of Dox and ELP-Dox conjugate treatment and the results are shown in Fig. 8. The results reveal that both the free drug and ELP-Dox conjugate are permeable to BMG-1 cerebral glioma cell line but show different intracellular uptake profiles. The control group (without the drug and the drug conjugate) does not show any drug uptake (Fig. 8a). The group treated with the free drug shows less drug uptake as compared to the group treated with ELP-Dox conjugate. The histogram of relative fluorescence per cell obtained from flow cytometry analysis and calculated relative fluorescence unit (RFU) of this distribution shows that the drug uptake by BMG-1 cerebral glioma cell line is more for ELP-Dox drug conjugate treated group as compared to free drug treated group (Fig. 8b).

The results of the RFU by flow cytometry are shown in Table 3. The results reveal an RFU of 100.7 for the free drug whereas when it is coupled to the ELP the RFU is 145 thus confirming that the drug uptake from ELP-Dox conjugate is more as compared to the free drug (Fig. 8c). The flow cytometry results thus reveal that the ELP synthesized is a good carrier for delivering drug to intracellular space.

Fig. 6: CD spectra of short ELP at selected temperatures namely, room temperature, 27⁰C, physiological temperature, 37⁰C and ITT and physical transition temperature, 40⁰C at a concentration of 100 µm in PBS at pH 7.2

The short ELP-Dox conjugate and Dox were assayed for their ability to inhibit the growth of BMG-1 cerebral glioma cell lines. Cells treated with the ELP, Dox, the ELP-Dox conjugate and the control (nontreated cells) were allowed to grow in 96 well plates and quantified by measuring crystal violet staining or cellular
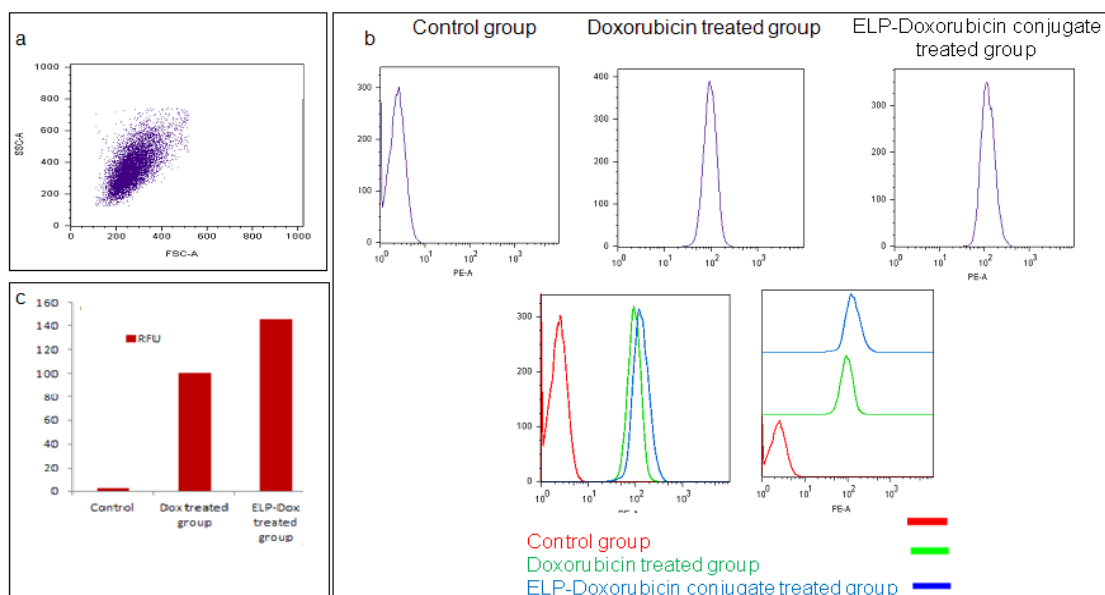

Fig. 8: a. Total cell population b. Flow cytometry histograms showing the relative fluorescence of BMG-1 cells after free drug, Dox and ELP-Dox conjugate treatment at 37⁰C. c. Total cellular uptake of drug treated and ELP-Dox conjugate treated group as expressed in RFU

Table 3: Cellular uptake measured by flow cytometry

Description	Concentration	Relative fluorescence unit (RFU)
Control group	100 μm	2.521 RFU
Dox treated group	100 μm	100.7 RFU
ELP-Dox conjugate treated group	100 μm	145.0 RFU

The autofluorescence of the Dox flouorophore allows to visualize differences in intracellular localization after exposure of cells to the free drug, Dox and ELP-Dox conjugate. The data obtained on Olympus BX 60 fluorescence microscope are shown in Fig. 9. The data reveal that the fluorescence distribution in BMG-1 cells exposed for 100 μm Dox and ELP-Dox conjugate at 4 and 24 h incubation. At both 4 h and 24 h incubation Dox accumulates at the nuclei whereas most of the ELP-Dox conjugate is located in either perinuclear region or cytoplasm initially with low fluorescence intensity. Further, on longer incubation a clear fluorescence localization was found for both the free drug as well as the drug conjugate. The results thus reveal that Dox targets the nucleus whereas the ELP-Dox conjugate targets distribution at the cytoplasm. Further, prolonged incubation of the free drug and ELP-Dox conjugate leads to more cellular uptake intensity. The low molecular weight free drug, Dox and the high molecular weight ELP-Dox conjugate thus show different cellular uptake mechanism.
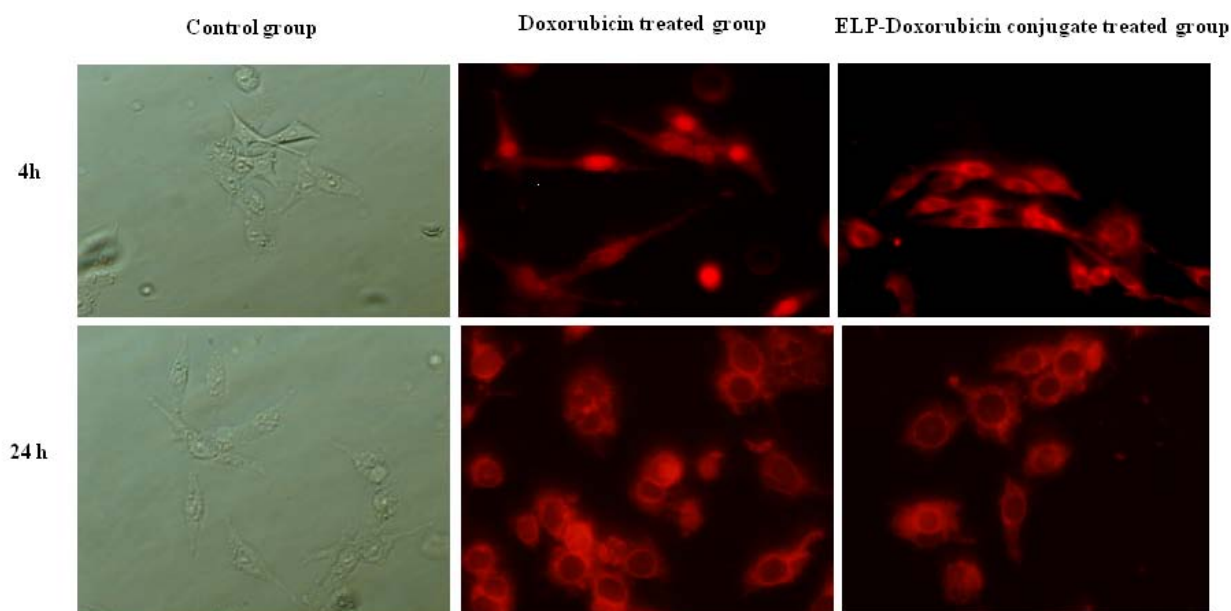

Fig. 9: Intracellular localization of free drug, Dox and ELP-Dox conjugate

CONCLUSION

The rationale for developing polymer-drug conjugate is to improve chemotherapy of anticancer drugs by overcoming some of their limitations. Our investigations reveal that a thermoresponsive short ELP-Dox conjugate can effectively deliver the anticancer drug, Dox to the intracellular space. Evidence for targeting specificity and cellular uptake of the drug from the ELP-Dox conjugate was obtained through confocal fluorescence microscopy and flow cytometry. It was also observed that coupling of Dox to the short ELP does not alter the toxicity profile of the drug. In summary, the present investigation clearly demonstrates that a short ELP is a good carrier for targeting anticancer drugs to the intracellular space. The present work should lead to newer polymeric drug conjugates for site-specific delivery of anticancer drugs with minimal side effects and thus improve cancer chemotherapy for human health.

The authors report no conflicts of interest.

ABBREVIATIONS

ax, axial; BMG-1, Cerebral glioma cell lines (BMG-1; wild-type p53); DHE, Dihydroethidium; DIC, N,N'-Diisopropylcarbodiimide; DMEM, Dulbecco's Modified Eagle Medium; Dox, Doxorubicin; ELP, Elastin like polypeptide; EPR, Enhanced permeability and retention; eq, equatorial; FACS, Fluorescence-activated cell sorting; Fmoc, Fluorenylmethyloxycarbonyl; G/Gly, Glycine; HoBt, Hydroxybenzotriazole; ITT, Inverse temperature transition; MTT, (3-(4,5-Dimethylthiazol-2-yl)-2,5-diphenyltetrazolium bromide; P/Pro, Proline; PBS, Phosphate Buffer Saline; RFU, Relative Fluorescence Unit; TFA, Trifluoroacetic acid; T_p, Peak temperature; V/Val, Valine

REFERENCES

1. Jain A, Jain A, Gulbake A, Hurkat P, Jain SK. Solid tumors: A review. Int J Pharm Pharm Sci 2011;3(5):45-51.
2. Duncan R. Polymer conjugates as anticancer nanomedicines. Nat Rev Cancer 2006;6(9):688-701.
3. Atkins JH, Gershell LJ. Selective anticancer drugs. Nat Rev Drug Discov 2002;1(7):491-2.
4. Huang PS, Oliff A. Drug-targeting strategies in cancer therapy. Curr Opin Genet Dev 2001;11(1):104-10.
5. Moses MA, Brem H, Langer R. Advancing the field of drug delivery: taking aim at cancer. Cancer Cell 2003;4(5):337-41.

6. Duncan R, Vicent MJ. Polymer therapeutics-prospects for 21st century: The end of the beginning. Adv Drug Deliv Rev 2013;65:60-70.
7. Meyer DE, Kong GA, Dewhirst MW, Zalutsky MR, Chilkoti A. Targeting a genetically engineered elastin-like polypeptide to solid tumors by local hyperthermia. Cancer Res 2001;61(4):1548-54.
8. Raucher D, Chilkoti A. Enhanced uptake of a thermally responsive polypeptide by tumor cells in response to its hyperthermia-mediated phase transition. Cancer Res 2001;61(19):7163-70.
9. Furgeson DY, Dreher MR, Chilkoti A. Structural optimization of a smart Doxorubicin polypeptide conjugate for thermally targeted delivery to solid tumors. J Control Rel 2006;110:362-9.
10. Bidwell GL, Davis AN, Fokt I, Priebe W, Raucher D. A thermally targeted elastin like polypeptide doxorubicin conjugate overcomes drug resistance. Invest New Drugs 2007;25:313-26.
11. Bidwell GL, Fokt I, Priebe W, Raucher D. Development of elastin like polypeptide for thermally targeted delivery of doxorubicin. Biochem Pharmacol 2007;73:620-31.
12. Dreher MR, Raucher D. Evaluation of an elastin like polypeptide-doxorubicin conjugate for cancer therapy. J Control Rel 2003;91:31-43.
13. Matsumura Y, Maeda A. A new concept for macromolecular therapeutics in cancer chemotherapy: mechanism of tumoritropic accumulation of proteins and the antitumor agent smancs. Cancer Res 1986;46(12):6387-92.
14. Langer R. Drug delivery and targeting. Nat 1998;392:5-10.
15. Jain RK. Delivery of novel therapeutic agents in tumors: physiological barriers and strategies. J Natl Cancer Inst 1989;81(8):570-6.
16. Jain RK. Delivery of molecular and cellular medicine to solid tumors. Adv Drug Deliv Rev 2001;46(1-3):149-68.
17. Nicolini C, Ravindra R, Ludolph B, Winter R. Characterization of the temperature and pressure induced inverse and reentrant transition of the minimum elastin like polypeptide GVG(VPGVG) by DSC, PPC, CD and FT-IR spectroscopy. Biophys J 2004;84:1385-92.
18. Nuhn H, Klok HA. Secondary structure formation and LCST behavior of short Elastin like peptides. Biomacromolecules 2008;9:2755-63.
19. Chabner BA, Longo DL. Cancer chemotherapy and biotherapy: principles and practice. New York, 3rd eds. Philadelphia: Lippincott Williams and Wilkins; 2001.
20. Saxena R, Nanjan MJ. A simple and efficient synthesis of 3-2 pyridinyldithio propanoic acid hydrazide: a heterobifunctional crosslinker. Int J Pharm Pharm Sci 2012;4(4):557-9.
21. Fields GB, Noble RL. Solid phase peptide synthesis utilizing 9-fluorenylmethoxycarbonyl amino acids. Int J Pept Protein Res 1990;35:161-214.